



CHORUS

This is the accepted manuscript made available via CHORUS. The article has been published as:

New measurement of the $E_{\alpha}^{\text{lab}}=0.83$ MeV resonance in $^{22}\text{Ne}(\alpha,\gamma)^{26}\text{Mg}$

Sean Hunt, Christian Iliadis, Art Champagne, Lori Downen, and Andrew Cooper

Phys. Rev. C **99**, 045804 — Published 24 April 2019

DOI: [10.1103/PhysRevC.99.045804](https://doi.org/10.1103/PhysRevC.99.045804)

New measurement of the $E_{\alpha}^{lab} = 0.83$ MeV resonance in $^{22}\text{Ne}(\alpha,\gamma)^{26}\text{Mg}$

Sean Hunt,^{1,2,*} Christian Iliadis,^{1,2} Art Champagne,^{1,2} Lori Downen,^{1,2} and Andrew Cooper^{1,2}

¹*Department of Physics & Astronomy, University of North Carolina at Chapel Hill, NC 27599-3255, USA*

²*Triangle Universities Nuclear Laboratory (TUNL), Durham, North Carolina 27708, USA*

(Dated: March 1, 2019)

The $E_{\alpha}^{lab} = 0.83$ MeV resonance in the $^{22}\text{Ne}(\alpha,\gamma)^{26}\text{Mg}$ reaction strongly impacts the reaction rates in the stellar temperature region crucial for the astrophysical s-process. We report on a new measurement of the energy and strength of this resonance using techniques different from previous investigations. We use a blister-resistant ^{22}Ne -implanted target and employ $\gamma\gamma$ -coincidence detection techniques. We find values for the resonance energy and strength of $E_{\alpha}^{lab} = 835.2 \pm 3.0$ keV and $\omega\gamma = (4.6 \pm 1.2) \times 10^{-5}$ eV, respectively. Our mean values are higher compared to previous values, although the results overlap within uncertainties. The uncertainty in the resonance energy has been significantly reduced. The spin-parity assignment, based on the present and previous work, is $J^{\pi} = (0^{+}, 1^{-}, 2^{+}, 3^{-})$.

I. INTRODUCTION

Knowledge of the $^{22}\text{Ne} + \alpha$ thermonuclear reaction rates is crucial for understanding the production of about half of the elements via neutron capture nucleosynthesis in the astrophysical s-process [1]. Neutron release in the $^{22}\text{Ne}(\alpha,n)^{25}\text{Mg}$ reaction also influences the relative production of ^{25}Mg and ^{26}Mg , whose abundance ratio can be measured to high precision in circumstellar (presolar) stardust grains that presumably originated from AGB stars [2]. The $^{22}\text{Ne}(\alpha,n)^{25}\text{Mg}$ rate also affects nucleosynthesis in type II supernova explosions [3] and in type Ia supernovae [4]. Besides the rate of the $^{22}\text{Ne}(\alpha,n)^{25}\text{Mg}$ reaction ($Q = -478.34 \pm 0.05$ keV), knowledge of the rate of the competing $^{22}\text{Ne}(\alpha,\gamma)^{26}\text{Mg}$ reaction ($Q = 10614.74 \pm 0.03$ keV [5]) is also important because the (α,γ) channel impacts the ^{22}Ne abundance, and thus the neutron production in the (α,n) channel. An extensive evaluation of the $^{22}\text{Ne} + \alpha$ rates was published by Longland, Iliadis and Karakas [6], while recent indirect measurements [7–9] have improved our understanding of the ^{26}Mg level structure in the astrophysically important range of excitation energies.

The $^{22}\text{Ne} + \alpha$ thermonuclear rates are still subject to large uncertainties that need to be reduced for reliable nucleosynthesis predictions. The present work addresses one particular aspect impacting the $^{22}\text{Ne} + \alpha$ rates, i.e., the strength of the lowest-energy resonance in the $^{22}\text{Ne}(\alpha,\gamma)^{26}\text{Mg}$ reaction. This resonance strongly impacts the reaction rates in the astrophysically significant temperature range between 200 MK and 1 GK. It was first observed by Wolke et al. [10] at $E_{\alpha}^{lab} = 828 \pm 5$ keV, with a strength of $\omega\gamma = (3.6 \pm 0.4) \times 10^{-5}$ eV. Gamma-ray branching ratios for primary transitions to the ^{26}Mg levels at 1809 keV and 7061 keV were also reported in Ref. [10]. The measured resonance energy corresponds to a ^{26}Mg excitation energy near $E_x = 11.3$ MeV. Because of the high level density above the α -particle threshold,

this resonance could correspond to a number of known ^{26}Mg levels populated in other reactions, as can be seen from Table IV in Ref. [7].

The strength of this resonance was measured by Wolke et al. [10] using an extended ^{22}Ne gas target and a small Ge(Li) γ -ray detector. Because of its outstanding importance for the reaction rates, we remeasured the resonance using different techniques. First, we employ an implanted ^{22}Ne target rather than a gas target, allowing for a straightforward determination of the resonance strength from the thick-target yield curve. Solid targets are usually destroyed quickly under α -particle bombardment because of blistering. In the present work, we employ a blister-resistant target, fabricated by implanting ^{22}Ne ions into a porous titanium structure. Second, the $^{22}\text{Ne}(\alpha,\gamma)^{26}\text{Mg}$ reaction has previously only been measured using singles spectroscopy. We employ a $\gamma\gamma$ -coincidence spectrometer, which is capable of detecting the entire cascade, thereby actively suppressing the ambient γ -ray background.

In Section II, we describe the experimental setup. Results are presented in Section III. A discussion and comparison to literature results are provided in Section IV. A summary is given in Section V.

II. EXPERIMENTAL SETUP

The measurements were performed at the Laboratory for Experimental Nuclear Astrophysics (LENA). Details about the facility can be found in Ref. [11]. In brief, a 1 MV model JN Van de Graaff accelerator delivered protons and singly-charged helium ions with a beam intensity of up to 100 μA on target. The proton beam was utilized to estimate the ^{22}Ne concentration in the targets (see below). The α -particle beam was energy-calibrated by measuring well-known narrow resonances in the $^7\text{Li}(\alpha,\gamma)^{11}\text{B}$ reaction [12]. The α -particle beam energy uncertainty amounted to ± 2 keV.

The ion beam entered the target chamber through a liquid-nitrogen cooled copper tube. An electrode was

* smhunt88@live.unc.edu

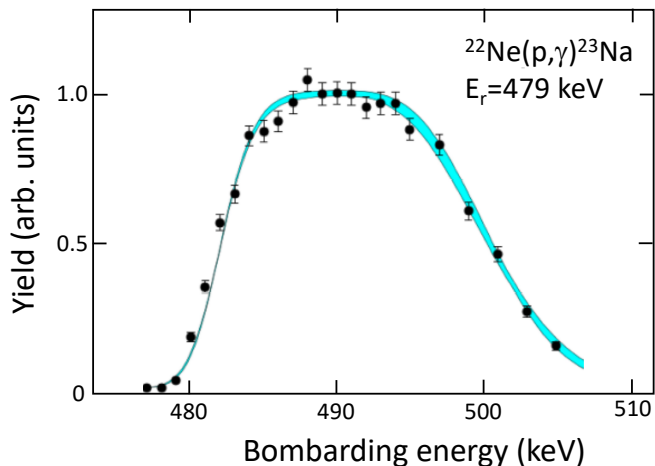


FIG. 1. (Color online) Yield curve for the $E_p^{lab} = 479$ keV resonance in the $^{22}\text{Ne}(p,\gamma)^{23}\text{Na}$ reaction, after an accumulated α -particle charge of 3.5 C. The γ -ray monitored for the yield had an energy of 6270 keV, corresponding to the $9252 \rightarrow 2982$ keV primary transition in ^{23}Na . The target thickness was about 19 keV for protons at this energy. The cyan shaded region depicts the uncertainty in the fitted yield curve.

mounted at the end of this tube and was biased to -300 V to suppress secondary electron emission. The target and chamber formed a Faraday cup for charge integration. The beam was focused and rastered into a circular profile of ≈ 12 mm diameter on target. The target was directly water cooled using de-ionized water.

In preparation for our experiment, ^{22}Ne -implanted targets were fabricated using multiple techniques. A detailed account of these efforts can be found in Hunt et al. [13]. For the present measurement we selected a porous titanium target. It was fabricated by evaporating a thick ($> 3 \mu\text{m}$) layer of titanium onto a 0.5-mm thick titanium backing. Subsequently, ^{22}Ne ions were implanted into the porous surface with an incident dose of ≈ 1 C. The incident ^{22}Ne -ion energy was 75 keV, corresponding to a target thickness of ≈ 95 keV for an α -particle beam of 828 keV energy [14]. During the (α,γ) experiment, the target did not show any visible signs of blistering or heat damage on the target surface. The target was frequently monitored using the $E_p^{lab} = 479$ keV resonance in $^{22}\text{Ne}(p,\gamma)^{23}\text{Na}$. A representative yield curve for the $9252 \rightarrow 2982$ keV primary transition in ^{23}Na is shown in Figure 1. The target stoichiometry was estimated from the maximum yield, using the value of the (p,γ) resonance strength from Kelly et al. [15]. The resulting stoichiometry, before any α -particle beam exposure, was $N_{Ti}/N_{^{22}\text{Ne}} = 3.8 \pm 0.6$. At the conclusion of the experiment, after a total accumulated α -particle charge of 4.4 C, the maximum yield had declined by 38%.

Gamma-rays were detected using LENA's $\gamma\gamma$ -coincidence spectrometer. The system contains a 135%-relative efficiency coaxial high-purity germanium (HPGe) detector, which was located at a distance of 1.1 cm to

the target, at an angle of 0° relative to the incident ion beam direction. The HPGe detector is surrounded by a NaI(Tl) annulus and a plastic (“veto”) scintillator shield [16]. Gamma-ray energy calibrations for both the HPGe and NaI(Tl) detectors were performed using well-known room-background peaks (^{40}K , ^{208}Tl), and γ -ray transitions from the $^{19}\text{F}(p,\alpha\gamma)^{16}\text{O}$ and $^{22}\text{Ne}(p,\gamma)^{23}\text{Na}$ reactions.

The spectrometer is capable of reducing the room background in the energy region below 2.6 MeV by several orders of magnitude. It is well characterized [17], allowing for the determination of reliable singles and coincidence detection efficiencies using GEANT4 simulations [18]. The pulse height spectra were modeled using a binned likelihood method with Monte Carlo simulated spectra (“templates”). The fraction of the experimental spectrum belonging to each template was obtained using a Bayesian statistical approach [19]. This allowed for the extraction of the primary γ -ray branching ratios and the total number of $^{22}\text{Ne}(\alpha,\gamma)^{26}\text{Mg}$ reactions. Corrections for coincidence summing are implicitly included in the Monte Carlo simulations used to generate the templates. The method assumes knowledge of the γ -ray branching ratios for secondary transitions in ^{26}Mg , which were adopted from Ref. [20]. Several different coincidence energy gates have been employed in the present work. One of the most useful gates accepted only events with $7.0 \text{ MeV} < E_\gamma^{HPGe} + E_\gamma^{NaI(Tl)} < 12.0 \text{ MeV}$ for the total energy deposited in the HPGe detector and NaI(Tl) annulus. The high-energy limit excludes cosmic-ray background with energies exceeding the excitation energy of the lowest-energy resonance in $^{22}\text{Ne}(\alpha,\gamma)^{26}\text{Mg}$, while the low-energy limit excludes events caused by room background and beam-induced background, e.g., $^{23}\text{Na}(\alpha,p\gamma)^{26}\text{Mg}$ ($Q = 1.82 \text{ MeV}$), $^{14}\text{N}(\alpha,\gamma)^{18}\text{F}$ ($Q = 4.41 \text{ MeV}$), $^{15}\text{N}(\alpha,\gamma)^{19}\text{F}$ ($Q = 4.01 \text{ MeV}$), and $^2\text{H}(n,\gamma)^3\text{H}$ ($Q = 6.26 \text{ MeV}$).

III. RESULTS

Data were accumulated at two bombarding energies, on resonance at $E_\alpha^{lab} = 904$ keV and off resonance at $E_\alpha^{lab} = 815$ keV, with accumulated charges of $Q = 3.4$ C and 1.4 C, respectively. Relevant parts of the HPGe pulse-height spectra, measured with α -particle beam incident on the ^{22}Ne -implanted Ti backing, are presented in Figure 2. The black and red histograms, both measured on resonance, show the singles and $\gamma\gamma$ -coincidence spectra, respectively. All peaks shown in the singles spectrum are caused by room background. None of these are present in the coincidence spectrum, which shows a single peak (not visible in the black histogram), corresponding to the secondary $1809 \rightarrow 0$ transition from the $^{22}\text{Ne}(\alpha,\gamma)^{26}\text{Mg}$ reaction. The blue histogram shows the off-resonance coincidence spectrum, where the peak at 1809 keV is absent.

We observed two primary transitions from the reso-

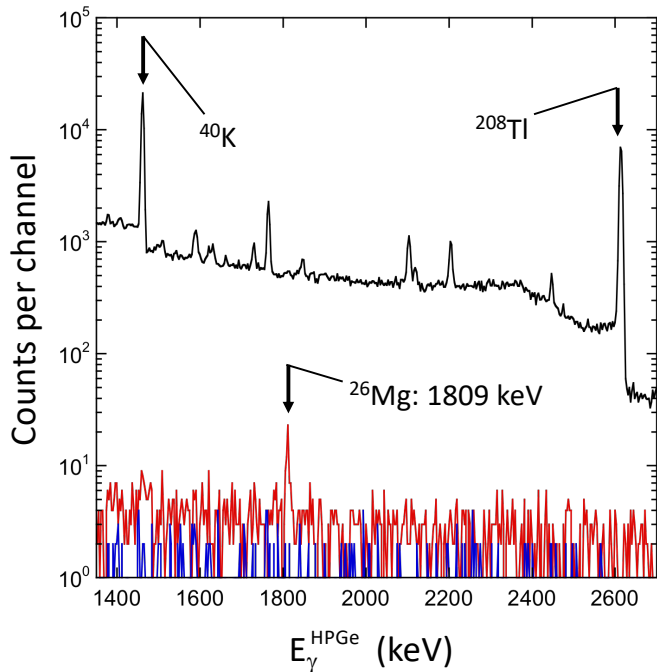


FIG. 2. (Color online) Selected parts of HPGe spectra, obtained with an α -particle beam on a ^{22}Ne -implanted Ti backing. (Black histogram) Singles spectrum at $E_{\alpha}^{lab} = 904$ keV (on-resonance), after a charge accumulation of 3.4 C; all peaks shown are caused by room background (^{40}K , ^{208}Tl , etc.). (Red histogram) $\gamma\gamma$ -coincidence spectrum with muon veto applied, recorded at the same energy and with the same charge accumulation; the secondary $1809 \rightarrow 0$ transition from the $^{22}\text{Ne}(\alpha,\gamma)^{26}\text{Mg}$ reaction is clearly observed. (Blue histogram) $\gamma\gamma$ -coincidence spectrum with muon veto applied, recorded at $E_{\alpha}^{lab} = 815$ keV (off-resonance) and a charge accumulation of 1.4 C. No contributions have been subtracted from any of the spectra shown.

nant level to final ^{26}Mg states at $E_x = 1809$ keV (2^+) and 7062 keV (1^-), as shown in the red histograms of Figure 3. Both transitions were reported previously [10]. These peaks are absent in the off-resonance run, shown as the blue histograms. Although both peaks are weak, the number of excess counts in the regions of interest is statistically significant. No other primary or secondary transitions were observed in the present work.

From the measured energies of the primary transitions, we estimated the excitation energy of the resonant level. Since it is located above both the α -particle and neutron thresholds, and can also γ -ray decay to many lower-lying states, it can be safely assumed that the γ -ray emissions occur at full velocity of the recoiling ^{26}Mg nucleus. After applying corrections for Doppler broadening, recoil shifts, and γ -ray attenuation coefficients, we find a weighted average value of $E_x = 11319.5 \pm 2.5$ keV (see Table I). Using the Q-value of Ref. [5], we derive laboratory and center-of-mass resonance energies of $E_{\alpha}^{lab} = 835.2 \pm 3.0$ and $E_{\alpha}^{cm} = 706.6 \pm 2.5$, respectively. Application of Endt's ‘‘Dipole or E2’’ rule [21], and taking

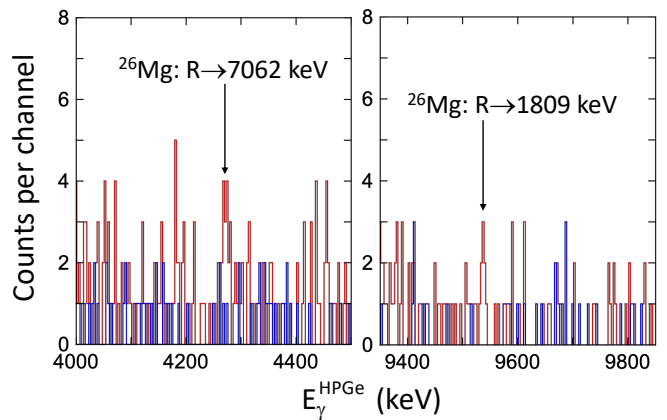


FIG. 3. (Color online) Selected parts of HPGe spectra, obtained with an α -particle beam on a ^{22}Ne -implanted Ti backing. The bombarding energies for the red and blue histograms were $E_{\alpha}^{lab} = 904$ keV (on-resonance) and 815 keV (off-resonance), respectively. The left panel shows $\gamma\gamma$ -coincidence spectra, while the right panel displays singles spectra with the muon veto applied. The two labeled peaks correspond to the only primary transitions in ^{26}Mg ($R \rightarrow 1809$ keV and $R \rightarrow 7062$ keV) observed during the experiment. No contributions have been subtracted from any of the spectra shown.

TABLE I. Results of present experiment and comparison to literature.

Quantity	Present	Previous ^a
E_x (keV)	11319.5 ± 2.5^b	$(11313.4 \pm 4.2)^c$
E_{α}^{lab} (keV)	835.2 ± 3.0^b	828 ± 5
E_{α}^{cm} (keV)	$(706.6 \pm 2.5)^d$	$(700.5 \pm 4.2)^d$
$B_{\gamma}^{R \rightarrow 1809}$ (%)	54 ± 12	47 ± 4
$B_{\gamma}^{R \rightarrow 7062}$ (%)	46 ± 12	53 ± 4
J^{π}	$(0^+, 1^-, 2^+, 3^-)^e$	1^- or 2^+^f
$\omega\gamma$ (eV)	$(4.6 \pm 1.2) \times 10^{-5}$	$(3.6 \pm 0.4) \times 10^{-5}$

^a From Ref. [10], unless noted otherwise.

^b From the measured energies of primary γ -ray transitions, including Doppler and recoil shift corrections.

^c Calculated from the reported laboratory resonance energy using the Q-value of Ref. [5].

^d Calculated from the reported laboratory resonance energy using the atomic masses of Ref. [5].

^e From application of ‘‘Dipole or E2’’ rule [21] to observed primary γ -ray decays.

^f The 1^- assignment was assumed for the reaction rate calculation in Ref. [10], while 2^+ was quoted in Refs. [6, 22]; both assignments are questionable (see text).

into account that only states of natural parity can be populated in the $^{22}\text{Ne} + \alpha$ reaction, yields spin-parity restrictions of $(0^+, 1^-, 2^+, 3^-)$ for the resonant level.

The resonance strength can be calculated from the experimental thick-target yield, according to [23]

$$\omega\gamma = \frac{2\epsilon_{eff}}{\lambda_r^2} \frac{N_R^{total}}{N_{\alpha}} \quad (1)$$

where N_α is the number of incident α -particles and λ_r is the de Broglie wavelength of the incident α -particle at the resonance energy. The effective stopping power, in the center-of-mass system, is given by

$$\epsilon_{eff} = \frac{M_{Ne}}{M_\alpha + M_{Ne}} \left(\epsilon_{Ne} + \frac{N_{Ti}}{N_{Ne}} \epsilon_{Ti} \right) \quad (2)$$

where M_α and M_{Ne} are the masses (in amu) of the projectile and target nuclei (^{22}Ne), respectively. The stopping cross sections in the laboratory system, ϵ_{Ne} and ϵ_{Ti} , were adopted from Ref. [14]. The initial target stoichiometry, N_{Ti}/N_{Ne} , is presented in Section II and was corrected for the observed target degradation. Application of the binned likelihood method (Section II) to relevant parts of our singles and coincidence pulse-height spectra containing secondary and primary transitions in ^{22}Mg provided the total number of reactions, $N_R = 4476 \pm 1081$, and the primary branching ratios, $B_\gamma^{R \rightarrow 1809} = 54 \pm 12\%$ and $B_\gamma^{R \rightarrow 7062} = 46 \pm 12\%$. The resulting resonance strength is $\omega\gamma = (4.6 \pm 1.2) \times 10^{-5}$ eV (Table I). The total uncertainty, obtained by adding statistical and systematic uncertainties quadratically, is dominated by counting statistics. Because of the close proximity of the target to the HPGe detector, and an almost full solid angle coverage of the NaI(Tl) annulus, corrections for possible γ -ray angular correlation effects are estimated to be much smaller than the quoted uncertainty.

IV. DISCUSSION

Table I compares our results to the values reported in Wolke et al. [10]. The only other measurement of the low-energy resonance in $^{22}\text{Ne}(\alpha,\gamma)^{26}\text{Mg}$ has been reported by Jaeger [24]. Jaeger's experiment was performed in the same laboratory as Wolke's, applied the same techniques (i.e., an extended ^{22}Ne gas target), and yielded similar results. Since his (α,γ) results have not been published, we will not discuss them further.

The uncertainty in our derived laboratory resonance energy is significantly smaller compared to the result reported by Ref. [10]. Our mean value is also higher by ≈ 7 keV, while present and previous results barely overlap within (68%) uncertainties. Koehler [25] argued that this $^{22}\text{Ne}(\alpha,\gamma)^{26}\text{Mg}$ resonance could not correspond to the $^{22}\text{Ne}(\alpha,n)^{25}\text{Mg}$ resonance observed at $E_\alpha^{lab} = 832 \pm 2$ keV by Jaeger et al. [26]. Although the argument for Koehler's claim has been refuted in Refs. [6, 7], the ^{26}Mg level density at this excitation energy is so high (see, e.g., Table IV in Ref. [7]) that it is not obvious how to unambiguously assign the resonant (α,γ) level to any state observed in other reactions.

Reported spin-parity assignments for the $E_x = 11.3$ MeV state are inconclusive as well. Wolke et al. [10] did not determine experimentally the spin-parity, but assumed a 1^- assignment for their reaction rate calculation. All that can be concluded from direct observation of the primary transitions is a spin-parity range of

$0^+, 1^-, 2^+, 3^-$ (see Table I). More recent work, e.g., Ref. [6], assigned a value of 2^+ to the (α,γ) resonance, based on the correspondence to a broad peak observed in the $^{22}\text{Ne}(^6\text{Li,d})^{26}\text{Mg}$ transfer experiment of Giesen et al. [22]. However, the observed deuteron peak could be easily caused by more than one level. Also, the $E_x = 11.3$ MeV level was not observed in the $^{26}\text{Mg}(\gamma,\gamma')^{26}\text{Mg}$ measurement of Longland et al. [27], which excited only dipole states ($J = 1$). This may be an argument against an 1^- assignment, but, again, the evidence is inconclusive.

Our primary branching ratios agree with those of Wolke et al. [10], although our uncertainties are larger. Present and previous values of the resonance strength agree within (68%) uncertainties, but our mean value is higher by $\approx 28\%$. Neither our resonance strength nor the value reported by Ref. [10] accounts for the unobserved primary transition to the ^{26}Mg ground state. From the single count observed in the region of interest, we estimated an upper limit strength of $\leq 9.7 \times 10^{-6}$ eV (97.5% coverage) for the ground state branch alone. Since this value is smaller than the uncertainty in our resonance strength (Table I), we disregarded this potential contribution.

V. SUMMARY

The $^{22}\text{Ne} + \alpha$ reactions are crucial for the astrophysical s-process. The $^{22}\text{Ne}(\alpha,\gamma)^{26}\text{Mg}$ reaction competes with the $^{22}\text{Ne}(\alpha,n)^{25}\text{Mg}$ neutron source. In the present work, we focused on the lowest-energy (α,γ) resonance, near $E_\alpha^{lab} = 0.83$ MeV, since the results of only a single measurement had been published previously. Therefore, we remeasured the resonance with a different γ -ray detection technique and a novel target. We find values for the resonance energy and strength of $E_\alpha^{lab} = 835.2 \pm 3.0$ keV and $\omega\gamma = (4.6 \pm 1.2) \times 10^{-5}$ eV, respectively. Both mean values are higher compared to the previous measurement, but the results agree within uncertainties. We reduced the uncertainty in the resonance energy significantly, although limited statistics prohibited us from improving the uncertainty in the resonance strength. Finally, the previously assumed unambiguous spin-parity assignments for this resonance (1^- or 2^+) have little experimental support. All that can be assigned based on the presently or previously observed γ -ray decay of this resonance is a spin-parity restriction of $(0^+, 1^-, 2^+, 3^-)$. New thermonuclear reaction rates based on the present and previously published results will be presented in a forthcoming publication.

ACKNOWLEDGMENTS

We would like to thank Robert Janssens and Richard Longland for providing helpful comments. This work was supported in part by the U.S. DOE under contracts

-
- [1] C. Sneden, J. J. Cowan, and R. Gallino, *Annual Review of Astronomy and Astrophysics* **46**, 241 (2008).
- [2] A. I. Karakas, M. A. Lugaro, M. Wiescher, J. Görres, and C. Ugalde, *Astrophysical Journal* **643**, 471 (2006).
- [3] M. Pignatari, R. Gallino, M. Heil, M. Wiescher, F. Käppeler, F. Herwig, and S. Bisterzo, *Astrophysical Journal* **710**, 1557 (2010).
- [4] F. X. Timmes, E. F. Brown, and J. W. Truran, *Astrophysical Journal Letters* **590**, L83 (2003).
- [5] M. Wang, G. Audi, F. G. Kondev, W. J. Huang, S. Naimi, and X. Xu, *Chinese Physics C* **41**, 030003 (2017).
- [6] R. Longland, C. Iliadis, and A. Karakas, *Physical Review C* **85**, 065809 (2012).
- [7] R. Talwar, T. Adachi, G. P. A. Berg, L. Bin, S. Bisterzo, M. Couder, R. J. deBoer, X. Fang, H. Fujita, Y. Fujita, J. Görres, K. Hatanaka, T. Itoh, T. Kadoya, A. Long, K. Miki, D. Patel, M. Pignatari, Y. Shimbara, A. Tamii, M. Wiescher, T. Yamamoto, and M. Yosoi, *Physical Review C* **93**, 211 (2016).
- [8] P. Adsley, J. W. Brümmer, K. C. W. Li, D. J. Marín-Lámbbari, N. Y. Kheswa, L. M. Donaldson, R. Neveling, P. Papka, L. Pellegrini, V. Pseudo, L. C. Pool, F. D. Smit, and J. J. van Zyl, *Physical Review C* **96**, 055802 (2017).
- [9] P. Adsley, J. W. Brümmer, T. Faestermann, S. P. Fox, F. Hammache, R. Hertenberger, A. Meyer, R. Neveling, D. Seiler, N. de Séréville, and H. F. Wirth, *Physical Review C* **97**, 045807 (2018).
- [10] K. Wolke, V. Harms, H. W. Becker, J. W. Hammer, K. L. Kratz, U. Schröder, H. P. Trautvetter, M. Wiescher, and A. Wöhr, *Zeitschrift fuer Physik A* **334**, 491 (1989).
- [11] J. M. Cesaratto, A. E. Champagne, T. B. Clegg, M. Q. Buckner, R. C. Runkle, and A. Stefan, *Nuclear Instruments and Methods A* **623**, 888 (2010).
- [12] F. Ajzenberg-Selove, *Nuclear Physics A* **506**, 1 (1990).
- [13] S. Hunt, C. Hunt, C. Iliadis, and M. Falvo, *Nuclear Inst. and Methods in Physics Research, A* **921**, 1 (2019).
- [14] J. Ziegler, “SRIM - Stopping Range of Ions in Matter,” <http://srim.org> (2013).
- [15] K. J. Kelly, A. E. Champagne, R. Longland, and M. Q. Buckner, *Physical Review C* **92**, 035805 (2015).
- [16] R. Longland, C. Iliadis, and A. Champagne, *Nuclear Instruments and Methods A* **566**, 452 (2006).
- [17] S. Carson, C. Iliadis, J. Cesaratto, A. Champagne, L. Downen, M. Ivanovic, J. Kelley, R. Longland, J. R. Newton, and G. Rusev, *Nuclear Instruments and Methods A* **618**, 190 (2010).
- [18] C. Howard, C. Iliadis, and A. Champagne, *Nuclear Instruments and Methods A* **729**, 254 (2013).
- [19] J. R. Dermigny, C. Iliadis, M. Q. Buckner, and K. J. Kelly, *Nuclear Instruments and Methods A* **830**, 427 (2016).
- [20] P. M. Endt, *Nuclear Physics A* **633**, 1 (1998).
- [21] P. M. Endt, *Nuclear Physics A* **521**, 1 (1990).
- [22] U. Giesen, C. Browne, J. Görres, S. Graff, and C. Iliadis, *Nuclear Physics A* **561**, 95 (1993).
- [23] C. Iliadis, *Nuclear Physics of Stars*, 2nd ed. (Wiley-VCH, Weinheim, Germany, 2015).
- [24] M. Jaeger, *Die Einfangreaktion $^{22}\text{Ne}(\alpha, n)^{25}\text{Mg}$ – die Hauptneutronenquelle in massiven Sternen*, Ph.D. thesis, Universität Stuttgart (2001).
- [25] P. E. Koehler, *Physical Review C* **66**, 055805 (2002).
- [26] M. Jaeger, R. Kunz, A. Mayer, J. W. Hammer, G. Staudt, K. L. Kratz, and B. Pfeiffer, *Physical Review Letters* **87**, 945 (2001).
- [27] R. Longland, C. Iliadis, G. Rusev, A. P. Tonchev, R. J. deBoer, J. Görres, and M. Wiescher, *Physical Review C* **80** (2009).